

# Supplement to Integrated epi-econ assessment: quantitative theory

TIMO BOPPART

Institute for International Economic Studies, Stockholm University and Department of Economics,  
University of Zurich

KARL HARMENBERG

Department of Economics, University of Oslo

JOHN HASSLER

Institute for International Economic Studies, Stockholm University

PER KRUSELL

Institute for International Economic Studies, Stockholm University

JONNA OLSSON

Department of Economics, NHH Norwegian School of Economics

## APPENDIX A: DETAILS ABOUT CALIBRATION

### A.1 *Detailed time use data*

Figure A.1 shows how young and old individuals divide their time between sleep, work, and leisure over time and how this has changed over time. As the figure shows, the changes over time are very small.

Figure A.2 shows how many minutes of the average working day is spent at home (112 minutes on average) and outside home, mainly at the workplace (255 minutes on average). As Figure A.2 also shows, there is no clear time trend in how large fraction of the working time that is spent at home. The slight downward trend in work done outside home can mainly be attributed to a compositional effect: the fraction of old individuals has increased slightly during this time period (21% in 2003 compared to 27% in 2018), and they work less, especially outside the home.

### A.2 *In-puBlic vs. in-priVate leisure*

This section provides more details on leisure time spent in the two categories in-puBlic (socially intense), and in-priVate (*not* socially intense).

---

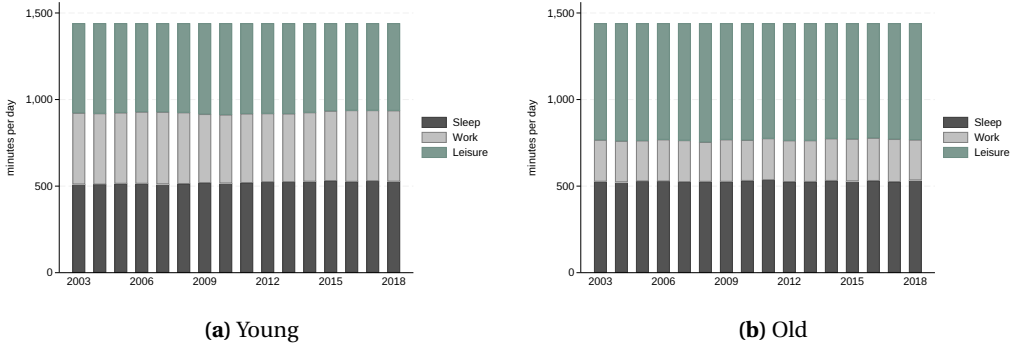
Timo Boppert: [timo.boppert@iies.su.se](mailto:timo.boppert@iies.su.se)

Karl Harmenberg: [karl.harmenberg@econ.uio.no](mailto:karl.harmenberg@econ.uio.no)

John Hassler: [john.hassler@iies.su.se](mailto:john.hassler@iies.su.se)

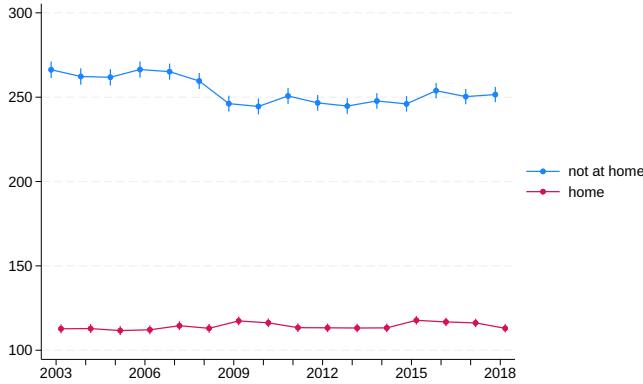
Per Krusell: [per.krusell@iies.su.se](mailto:per.krusell@iies.su.se)

Jonna Olsson: [jonna.olsson@nhh.no](mailto:jonna.olsson@nhh.no)



A full day is  $24 \cdot 60 = 1,440$  minutes.  
Source: ATUS.

FIGURE A.1. Time spent on sleep, work, and leisure over time.



Source: ATUS.

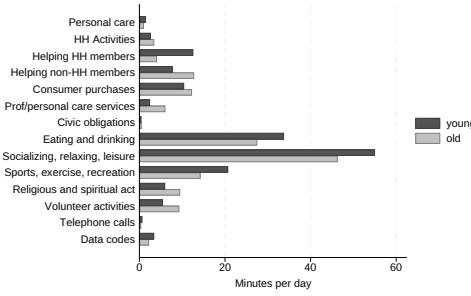
FIGURE A.2. Average minutes per day spent working home vs. not from home.

We classify activities as *not* socially intense if it took place in the respondent’s home or yard. Moreover, we classify personal care activities (e.g., grooming and personal activities) coded with location code “Blank” in the survey as not socially intense. Lastly, 0.3% of the observations in the data are coded with “Unspecified place”. For these observations, we code those where it is plausible that the activity took place in the home as not socially intense.<sup>1</sup>

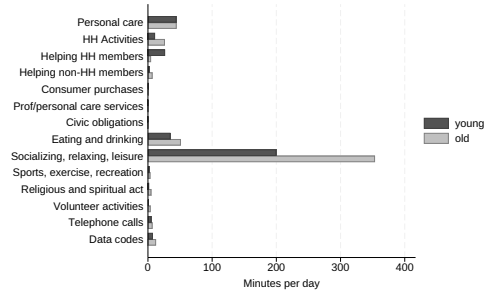
The socially intense activities are consequently the activities that took place outside home. Examples of locations for these activities include someone else’s home, store/mall, restaurant or bar, and gym/health club.

To understand what these broad categorizations mean in practice, Figure A.3 shows socially intense leisure and not-socially-intense leisure broken down on a finer level. For

<sup>1</sup>As an example, we code the activity “Caring for and helping household children” as not socially intense, while “Participating in sports” is classified as socially intense.



(a) Socially intense in-public leisure



(b) Not socially intense in-private leisure

“Data codes” refer to observations where the respondent couldn’t remember or refused to answer. A full day is  $24 \cdot 60 = 1440$  minutes. Source: ATUS, 2018.

FIGURE A.3. Average minutes per day spent in socially intense leisure activities and not socially intense activities, by two-digit categories (includes associated traveling).

instance, the category “Eating and drinking” shows up in both types of leisure: young spend on average 34 minutes per day eating and drinking outside their home (socially intense in-public leisure), and 35 minutes on eating and drinking at home (not-socially-intense in-private leisure). The largest category for leisure is “Socializing, relaxing, and leisure”, both when it comes to socially intense leisure and not-socially-intense leisure. On a finer classification level, the most common subcategory within “Socializing, relaxing, and leisure” for the in-public type is “Socializing and communicating”, while it for the in-private type is “Relaxing and leisure”, which roughly translates to watching television at home.

### A.3 Sector classification

Table A.1 gives an example of how different sectors are classified as being fully, to a high extent, somewhat, or not at all employing people who are in social contact with customers.

#### A.4 Robustness of choice of outer elasticity

To get more insights on how the outer elasticity in the nested CES utility function,  $\varepsilon$ , impacts the time allocations in a model with a pandemic, we evaluate how the optimal time allocations of the young and old vary with the cost of an infection, using different values of  $\varepsilon$ .

Recall that the flow utility for an individual is given by

$$u(c_B, h_B, c_V, h_V) = \log \text{CES}(\tilde{c}_B, \tilde{c}_V; \lambda, \varepsilon) + \underline{u}, \tag{1}$$

$$\tilde{c}_B = \text{CES}(c_B, h_B; \lambda_B, \varepsilon_B), \tag{2}$$

$$\tilde{c}_V = \text{CES}(c_V, h_V; \lambda_V, \varepsilon_V). \tag{3}$$

TABLE A.1. Illustrative example of sector classification.

2017 NAICS	Description	Employees Thousands	Active sector production?
211	Oil and gas extraction	683.3	No
...			
441	Motor vehicle and parts dealers	2,021.2	No
445	Food and beverage stores	3,087.1	High extent
452	General merchandise stores	3,104.9	High extent
...			
711	Performing arts, spectator sports, and related industries	506.0	Yes
...			
7131	Amusement parks and arcades	211.0	Yes
7132	Gambling industries (except casino hotels)	120.4	High extent
...			
721	Accommodation	2,028.4	Yes
722	Food services and drinking places	11,926.3	Yes
...			
8121	Personal care services	727.8	Yes
8122	Death care services	137.1	No
...			
-	Non-agriculture self-employed	9,453.4	Somewhat
<b>Total number of employees</b>		161,037.7	

The nested CES structure captures that to consume a good, both social and non-social, involves spending time with the good.

For concreteness, assume that eight percent of the population is infected, and the rest is susceptible. The infected are evenly spread out in the young and the old population. Moreover, assume that the cost of an infected old is 50 times the cost of an infected young (this might sound high, but as shown in the full dynamic model this outcome is not at all extreme compared to the outcome in the rational expectations competitive equilibrium).

Figure A.4 shows the time allocations for the young and the old as a function of the cost of a young infection for our baseline scenario  $\varepsilon = 1.0$ . As the cost of infections increases, individuals reallocate their time. In this example, very soon the old stop working in the workplace and all work is done from home. They also gradually reduce their in-public leisure time.

In Figure A.5 we show the corresponding graphs from the same experiment, but setting  $\varepsilon = 0.4$ .<sup>2</sup> Here we see that the reallocation pattern for the old is qualitatively different. When it becomes very costly to be infected, they cut down on work in the workplace first, just as before. Then the old cut down on leisure in-public, also as before. However, with an elasticity below one, the composite in-public good and the composite in-private good are complements, and therefore the marginal utility from in-private leisure falls. Thus, if the old are prevented from enjoying in-public leisure, their time spent watching TV will eventually fall as well. This implication we argue is implausible, and therefore advice against an  $\varepsilon < 1$ .

Figure A.6 shows the same experiment setting  $\varepsilon = 1.3$ . The in-public and the in-private composite goods are now substitutes, and thus the reallocation from in-public leisure to in-private leisure is somewhat stronger than in our base case. However, the

<sup>2</sup>Using another outer elasticity means that we also have to recalibrate the other remaining parameters, which we also do.

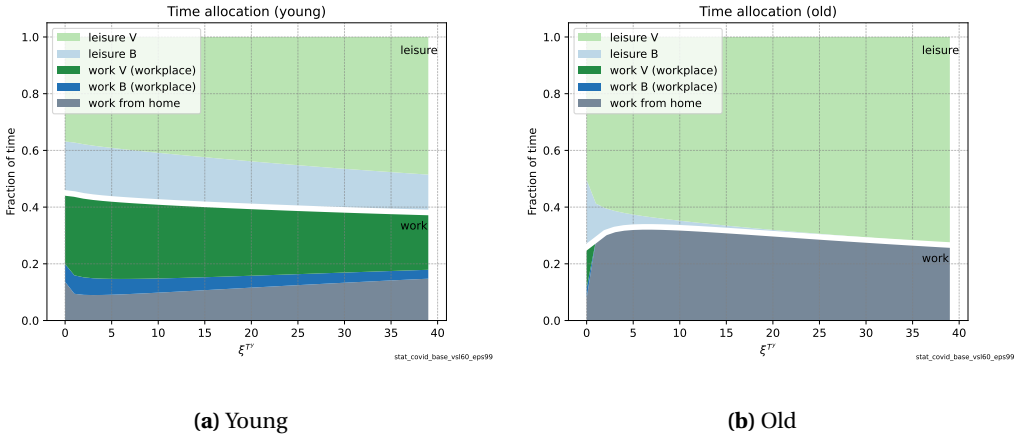


FIGURE A.4. Time allocations as a function of the cost of new infections with  $\varepsilon = 1.0$  under the assumption that eight percent of the population is infected and the remaining population susceptible. The cost of a new infection for the old is assumed to be 50 times as large as the cost for the young,  $\xi^{T^o} = 50\xi^{T^y}$ .

difference compared to our base case is relatively small and does not translate into any meaningful difference in results from the full model, as we show in the next subsection.

**A.4.1 Baseline scenario with a higher outer elasticity** To get a better understanding of how the results differ in the baseline scenario if we choose a higher outer elasticity we run the baseline with a higher value of  $\varepsilon$  and contrast the results to the main specification with  $\varepsilon$  set to unity.

Figure A.7 shows the time allocation of the old in two versions of the competitive equilibrium in the baseline scenario: subfigure A.7a shows the case with  $\varepsilon = 1.0$  (in which  $\log(\tilde{c}_B^i)$  and  $\log(\tilde{c}_V^i)$  are additively separable) and subfigure A.7b shows the case with  $\varepsilon = 1.8$  (thus with imperfect substitutability between the  $\tilde{c}_B^i$  and  $\tilde{c}_V^i$ ). Figure A.7a thereby replicates Figure 3b in the main paper. We focus on the behavior of the old, since the previous subsection showed that the behavior of the young is much less affected and changes less during the epidemic.

When the two composite goods are (imperfect) substitutes, the old agents choose to isolate themselves to a higher extent during the peak of the epidemic, and spend virtually all leisure time on the in-private type during the peak of the epidemic. However, with higher substitutability between the two composite goods the utility cost from shielding is lower, which is shown in Figure A.8. Subfigure A.8a shows the flow utility during the course of the epidemic in the case of  $\varepsilon = 1.0$  (replicating Figure 6a in the main paper) while subfigure A.8b shows the case of  $\varepsilon = 1.8$ . As the figures show, the utility loss for the old is not as severe in the case of  $\varepsilon = 1.8$ , even though the main picture remains: the old suffer more than the young during the epidemic.

For the planner, the differences are less stark. Figure A.9 shows corresponding graphs for the planner solution, and as the figures show, the planner does reallocate the time

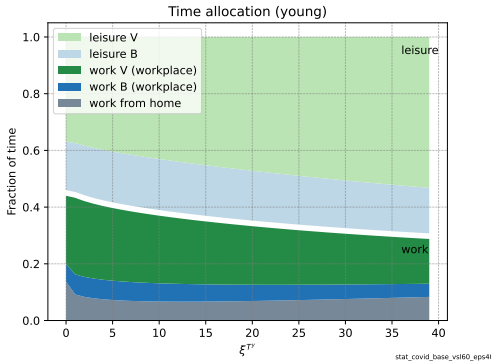
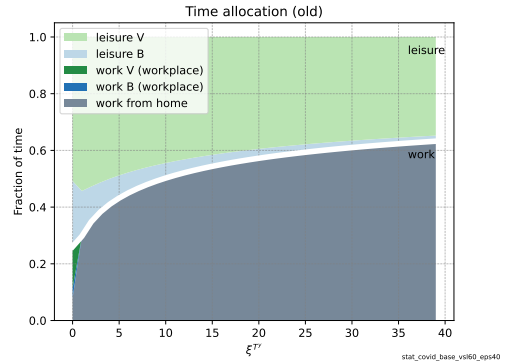
(a) Young,  $\varepsilon = 0.4$ .(b) Old,  $\varepsilon = 0.4$ .

FIGURE A.5. Time allocations as a function of the cost of new infections with  $\varepsilon = 0.4$  under the assumption that eight percent of the population is infected and the remaining population susceptible. The cost of a new infection for the old is assumed to be 50 times as large as the cost for the young,  $\xi^{T^o} = 50\xi^{T^y}$ .

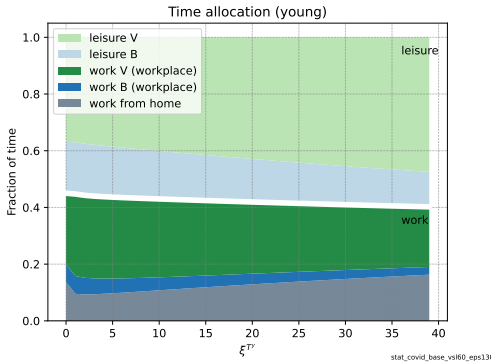
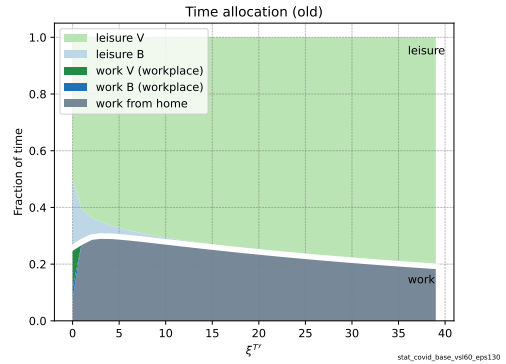
(a) Young,  $\varepsilon = 1.3$ .(b) Old,  $\varepsilon = 1.3$ .

FIGURE A.6. Time allocations as a function of the cost of new infections with  $\varepsilon = 1.3$  under the assumption that eight percent of the population is infected and the remaining population susceptible. The cost of a new infection for the old is assumed to be 50 times as large as the cost for the young,  $\xi^{T^o} = 50\xi^{T^y}$ .

spent in the different types of leisure, but not as much. In the planner scenario, the optimal allocation is still to let the old enjoy both in-private and some in-public leisure also during the peak of the epidemic.

Consequently, the infection curves for the planner look very similar for the two choices of  $\varepsilon$ , the elasticity between the  $\tilde{c}_B^i$  and  $\tilde{c}_V^i$  bundles. Figure A.10 shows the infection curves for the planner allocations in the two cases, and as can be seen, the planner still adopts a “protect the healthcare system” strategy.

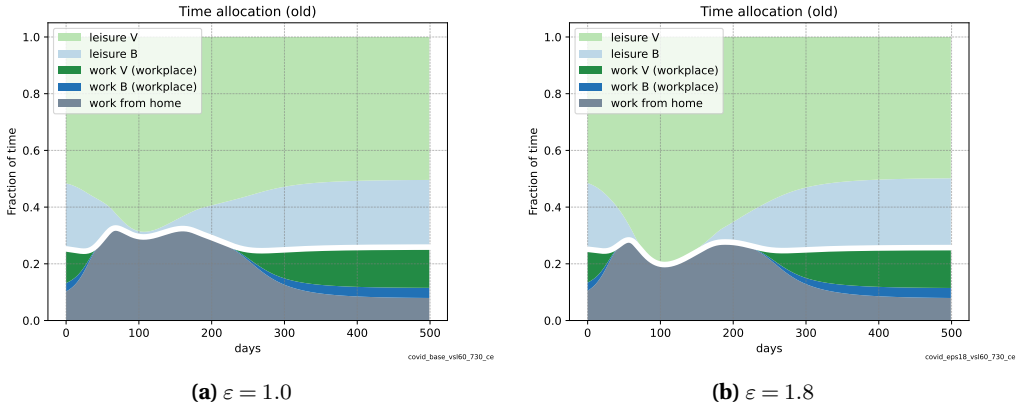


FIGURE A.7. Time allocation in rational-expectation competitive equilibrium for the old, baseline scenario. Contrasting two cases with different elasticity between the  $\tilde{c}_B^i$  and  $\tilde{c}_V^i$  bundles.

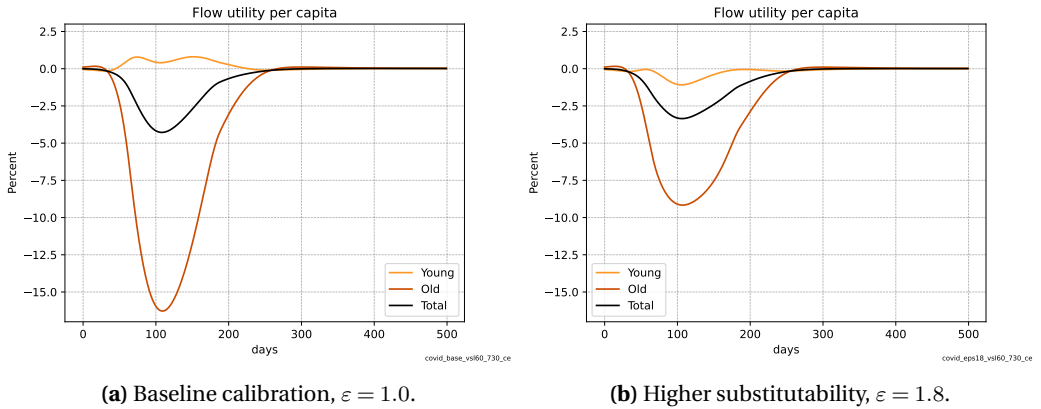


FIGURE A.8. Flow utility in the rational-expectations competitive equilibrium, baseline scenario. Contrasting two cases with different elasticities between the  $\tilde{c}_B^i$  and  $\tilde{c}_V^i$  bundles.

In general, the main insights from the model remain even with a higher substitutability between the in-public and in-private bundles, even though the precise allocations for both the rational-expectations scenario and the planner solution change slightly, as shown in this section. Also the exact thresholds for when the planner solutions qualitatively shift (for instance precisely which severity of overcrowding of the hospitals that is required for the planner to induce a speed-up-the-infection strategy, or how soon the cure must be expected to induce a lock-down), depends on the substitutability but the trade-offs and insights remain. Clearly, with an extremely high substitutability between the in-public and in-private consumption/leisure bundles, the picture would be different and the insights may change more drastically. However, the difficulty in practice during the Covid-19 epidemic to get people to stay at home shows that a close to perfect substitutability does not seem to be the empirically relevant case.

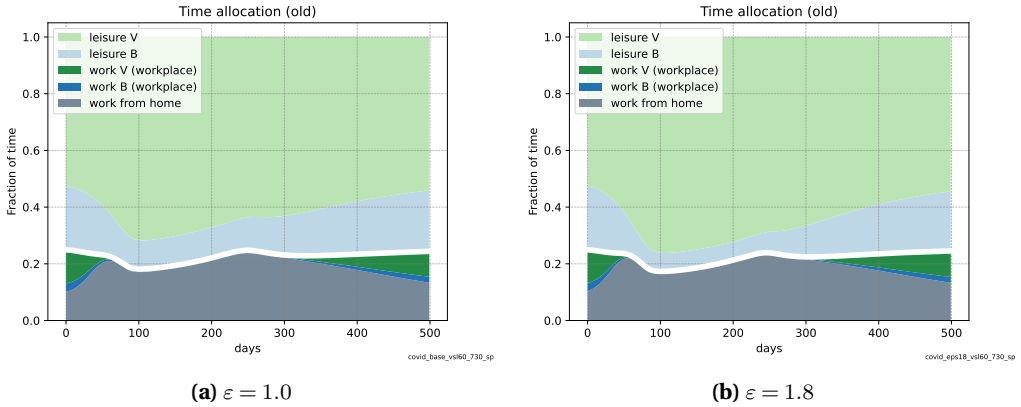


FIGURE A.9. Time allocation in the planner solution for the old, baseline scenario. Contrasting two cases with different elasticity between the  $\tilde{c}_B^i$  and  $\tilde{c}_V^i$  bundles.

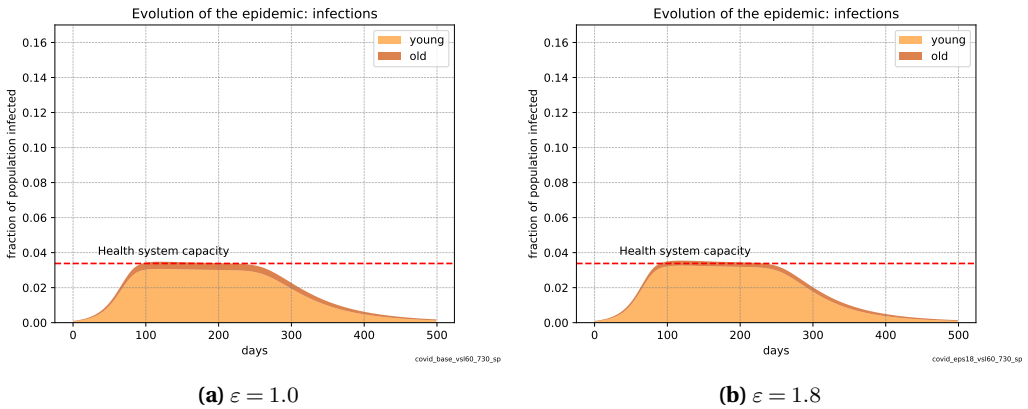


FIGURE A.10. The evolution of the epidemic (fraction of population currently infected) in the planner solution. Contrasting two cases with different elasticity between the  $\tilde{c}_B^i$  and  $\tilde{c}_V^i$  bundles.

### A.5 Calibration of elasticities

To pin down our choice of  $\varepsilon_B$  and  $\varepsilon_V$ , the elasticities for the consumption-leisure bundle in the socially intense B sector and the non-social V-sector respectively, we put the two following restrictions on our utility function: a) the income effect should dominate the substitution effect in a realistic way, and b) the young should spend a larger fraction of their leisure in the socially intense B activity. These two restrictions narrow down the set of  $\varepsilon_B/\varepsilon_V$  we can choose from substantially. Figure A.11 shows a number of combinations of elasticities that satisfies those two restrictions. In the graph, combinations that lie “south-east” of the marked area are combinations for which the second requirement is not fulfilled.

As our base case, we pick  $\varepsilon_B = 0.41$  and  $\varepsilon_V = 0.8$ , but note that for basically all permissible combinations, we have that  $\varepsilon_B < \varepsilon_V$  and both elasticities being smaller than



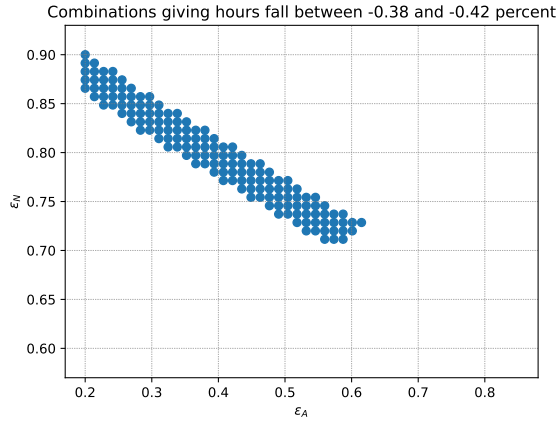


FIGURE A.11. Combinations of  $\varepsilon_B$  and  $\varepsilon_V$  that satisfy both criterion a) and b). Criterion a) A realistic income/substitution effect is defined as if a TFP increase of 2% leads to hours worked falling by between 0.38 and 0.42 percent. Criterion b) Young spend a larger fraction of their leisure time in the socially intense type than the old do.

1. This means that for any of the combinations we could choose as an alternative, the model behaves extremely similar and no insights of the working of the economy change.

To understand why these elasticities affect how leisure is distributed between the socially intense  $B$  type and the not-social  $V$  type, think about a marginal increase in leisure: how should it be split up between the two types of leisure? The answer is of course so that the marginal utilities of the two types still are equalized. The marginal utility with respect to the socially intense  $B$  type of leisure is given by:

$$\begin{aligned} u_{h_B} &= \frac{\partial u}{\partial \tilde{u}_B} \cdot \frac{\partial \tilde{u}_B}{\partial h_B} \\ &= \frac{\partial u}{\partial \tilde{u}_B} \cdot \left( \lambda_B c_B^{\frac{\varepsilon_B-1}{\varepsilon_B}} + (1-\lambda_B) h_B^{\frac{\varepsilon_B-1}{\varepsilon_B}} \right)^{\frac{1}{\varepsilon_B-1}} (1-\lambda_B) h_B^{-\frac{1}{\varepsilon_B}} \end{aligned}$$

Thus, the elasticity of the marginal utility with respect to leisure ( $i \in \{B, V\}$ ):

$$\begin{aligned} \frac{d \log u_{h_i}}{d \log h_i} &= \frac{d}{d \log h_i} \left[ \log \frac{\partial u}{\partial \tilde{u}_i} + \log(1-\lambda_i) \right. \\ &\quad \left. + \frac{1}{\varepsilon_i-1} \log \left( \lambda_i c_i^{\frac{\varepsilon_i-1}{\varepsilon_i}} + (1-\lambda_i) h_i^{\frac{\varepsilon_i-1}{\varepsilon_i}} \right) - \frac{1}{\varepsilon_i} \log h_i \right] \\ &= \frac{1}{\varepsilon_i} \left( \frac{(1-\lambda_i) h_i^{\frac{\varepsilon_i-1}{\varepsilon_i}}}{\lambda_i c_i^{\frac{\varepsilon_i-1}{\varepsilon_i}} + (1-\lambda_i) h_i^{\frac{\varepsilon_i-1}{\varepsilon_i}}} \right) - \frac{1}{\varepsilon_i} \end{aligned}$$

$$= -\frac{1}{\varepsilon_i} \left( 1 - \frac{(1 - \lambda_i) h_i^{\frac{\varepsilon_i - 1}{\varepsilon_i}}}{\lambda_i c_i^{\frac{\varepsilon_i - 1}{\varepsilon_i}} + (1 - \lambda_i) h_i^{\frac{\varepsilon_i - 1}{\varepsilon_i}}} \right)$$

Hence, the elasticity of the marginal utility with respect to leisure depends on the CES elasticity (and the consumption/leisure terms within the respective bundles). The relative size of the terms in the bundles are primarily determined by the other exogenously set calibration targets and do not depend on  $\varepsilon_i$  to any larger extent. The relationship between  $\varepsilon_B$  and  $\varepsilon_V$  is therefore crucial for determining where to spend a marginal increase in leisure. With  $\varepsilon_B < \varepsilon_V$ , a marginal increase in leisure is spent proportionally more on the not-social  $V$  good (had the bundles been exactly the same).

## APPENDIX B: ADDITIONAL RESULTS

### B.1 *Time allocations from the extended model*

Figure B.1 shows the time allocations in the rational expectations competitive equilibrium from the extended model with waning immunity, exogenous seasonality, and three types. As can be seen, the young do not adjust their behavior to any larger extent, while the old and the very old do. The old shifts to working at home and only have in-private leisure, while the very old are so unproductive that they do not work, but only cut down on in-public leisure.

Figure B.2 shows the corresponding graphs for the planner's allocation. In this scenario, the young adjust their time to a larger extent, and cut down on their time in the workplace and in-public leisure. This allows for more in-public leisure for the old and the very old.

### B.2 *Flu simulations, more details*

To simulate a “seasonal flu” we set the basic reproduction number,  $R_0$ , to 1.3, use a death rate of 0.00045, and a recovery rate of 1/10. This corresponds to a regular normal flu season, and not to a year with a particularly severe instance of the flu, or a year with a pandemic influenza (such as the H1N1/09 virus in 2009).

A systematic review of several published estimates of the basic reproduction number for the seasonal influenza, conducted by Biggerstaff et al. (2014), found that the median estimate of  $R_0$  for the seasonal flu was 1.3, so we use this number directly.

The infection fatality rate for a seasonal flu is more difficult to estimate, and it also varies substantially from year to year. A commonly cited case fatality rate for the seasonal flu is 0.1% (Faust and Del Rio (2020)). According to WHO, the infection fatality rate (i.e., the proportion of deaths among all infected individuals, including all asymptomatic and undiagnosed subjects) is usually well below 0.1%.<sup>3</sup> In order to be conservative, we set the infection fatality rate to less than half of this: 0.045%. An important difference between a regular influenza and covid-19 is also how different groups in the

<sup>3</sup>See <https://www.who.int/news-room/q-a-detail/coronavirus-disease-covid-19-similarities-and-differences-with-influenza>, downloaded 2020/10/27.

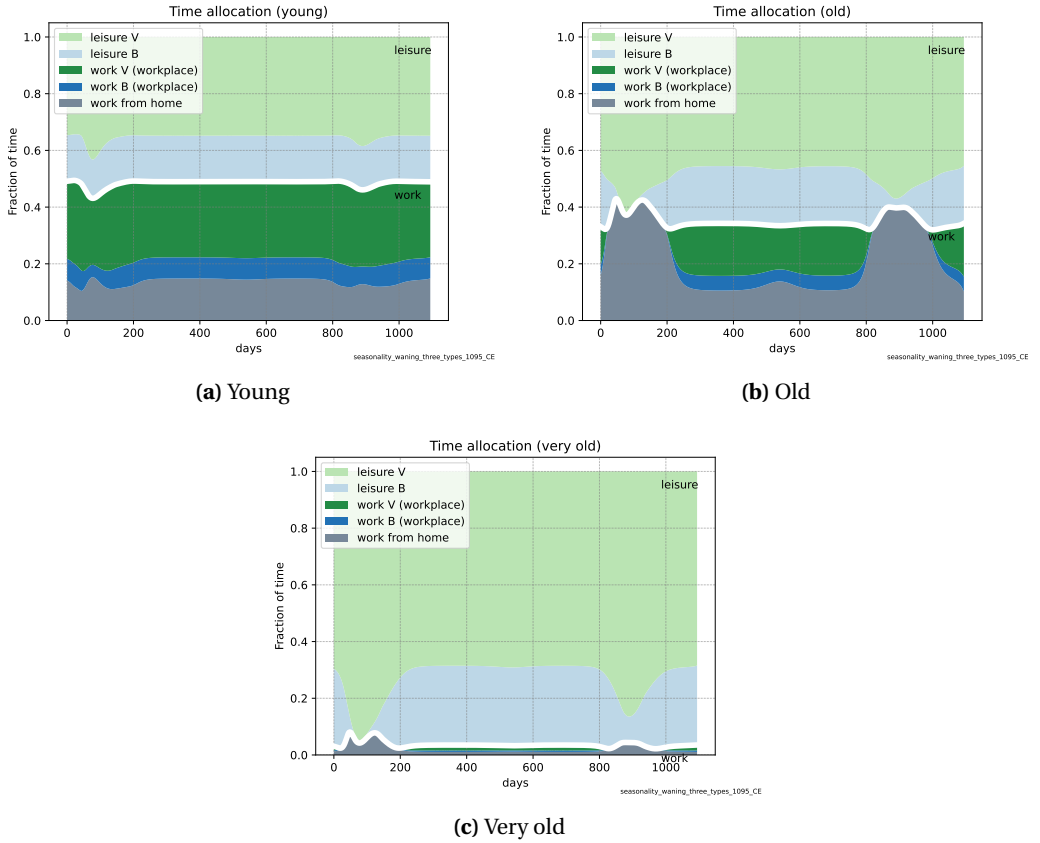


FIGURE B.1. Time allocation in the competitive equilibrium, extended model.

population are affected. According to [Petersen et al. \(2020\)](#), 80% of the deaths from the pandemic influenza in 2009 were work below the age of 65, but for a seasonal flu the deaths are more skewed towards the elderly, but not as much as for covid-19. We set an equal death rate for the young and for the old as defined in our model.

According to [Petersen et al. \(2020\)](#), the proportion of infected individuals requiring intensive care is also substantially lower for a pandemic influenza than for covid-19 (less than a sixth). We do not observe any particular overcrowding problems in hospitals during a seasonal flu. To be conservative, we choose to remove the overburdening of the healthcare system effect, and have the same death rate regardless of the number of infected in the economy.

Further, we assume that on average it takes less time to recover from a flu than from covid-19. For the flu, we use 10 days to recover on average.

To ensure that our estimates of the reproduction number, the infection fatality rate, and estimated time for recovery are plausible, we simulate the myopic model and the rational expectation model to see what the model predicts in terms of deaths. The result is 1.9 (myopic) or 1.8 (rational expectations) deaths per 10,000 people, which rescaled

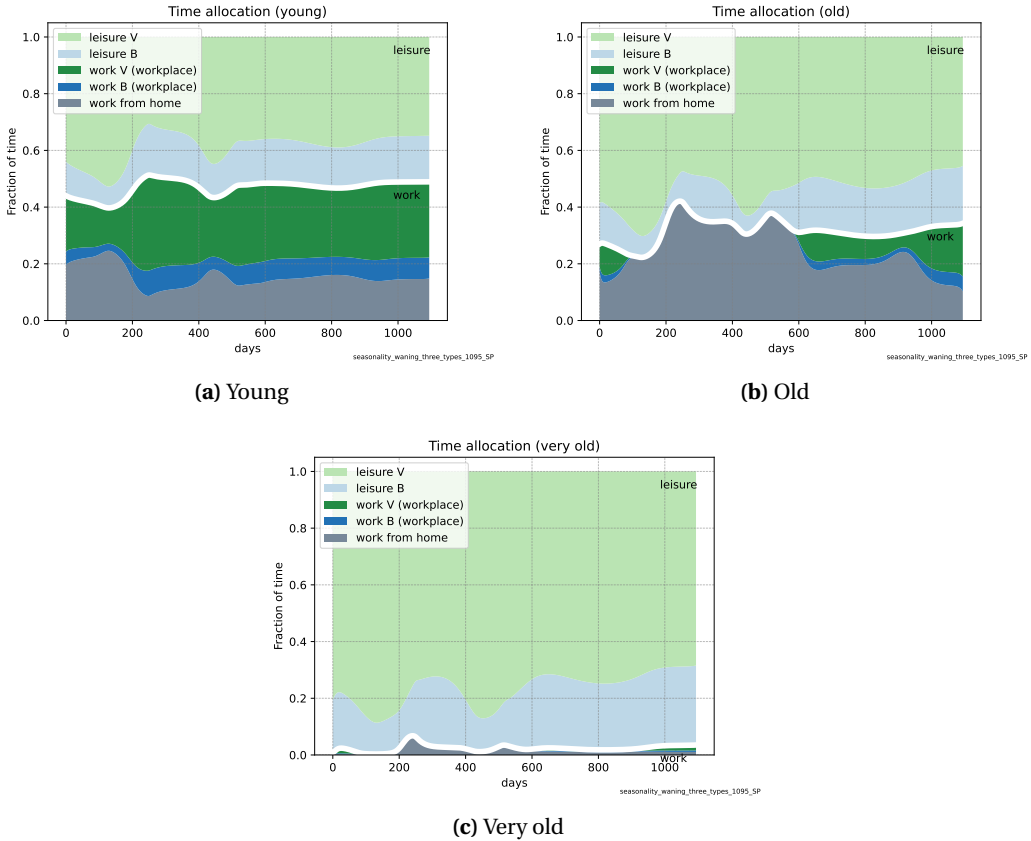


FIGURE B.2. Time allocation in the planner's solution, extended model.

to the full population is 1.5 (myopic) and 1.4 (rational expectations) deaths per 10,000 people.<sup>4</sup>

Rolfes et al. (2018) estimate the burden of seasonal influenza in the US and find that the annual deaths due to the seasonal flu in the period between the 2010/2011 season and the 2015/2016 season can have varied between 16,000 and 76,000. Using the average of this low and high number (and approximating the US population to 320 million) gives us a death toll of 1.4 per 10,000 individuals. Another estimate is given by Dushoff et al. (2006), who find an annual average number of deaths in the US from influenza of 41,400 over the period 1979 to 2001. Approximating the US population to 280 million (approximate average during this time period) gives 1.5 deaths per 10,000. A third set of estimates of the total number of deaths per year due to the seasonal flu is provided by CDC.<sup>5</sup> The median of their estimated number of deaths for the period 2010/2011 to 2018/2019 is 1.2 deaths per 10,000 people. Compared to these numbers, our simulated flu is slightly worse than the median flu, but not as severe as for instance the 2014/2015 flu (with 1.6

<sup>4</sup>Our model does not include individuals below the age of 15, who constitute 21.4% of the population. We assume for simplicity that there are no deaths in this group.

<sup>5</sup>See <https://www.cdc.gov/flu/about/burden/index.html>, downloaded 2020/10/21.

deaths per 10,000) or the 2017/2018 flu (with 1.9 deaths per 10,000). Hence, our implied estimate of 1.4 – 1.5 deaths per 10,000 people during a normal flu year seems to be well in line with what is observed .

In sum, the flu we simulate corresponds to a reasonably normal seasonal flu, and not a year with a particularly severe flu. It is also far from a pandemic influenza such as the 2009 case. Note also that we do not take into account the burden of a seasonal flu in terms of people being sick and having to stay at home in bed for days.

*Results seasonal flu* Figure B.3 compare the number of deaths, the output loss and the flow utility loss for a seasonal flu in the myopic market allocation, the rational-expectations competitive equilibrium, and the social planner's allocation, assuming the lower value of a statistical life. Figure B.5 shows the evolution of infected individuals in the three scenarios, and as the figures show, the evolution is very similar across scenarios.

A social planner would want to decrease output by 1.9 percent during the second quarter of the epidemic, as can be seen in Figure B.3b, and the annual drop in output is 1.1 percent. However, this translates into a smaller fall in flow utility, as Figure B.3c shows.

Figure B.4 shows the corresponding results assuming the higher estimate for the value of a statistical life. With the high value of a statistical life, the social planner would want to lower output by 4.0 percent during the second quarter, and the annual drop in output is 2.8 percent. This, as far as we can tell, is not how actual policy makers have reacted historically. Thus, although we cannot say whether a chosen value of a statistical life is the correct one, the results from the flu simulations indicate that a value from the lower range is more in line with observed policy actions.

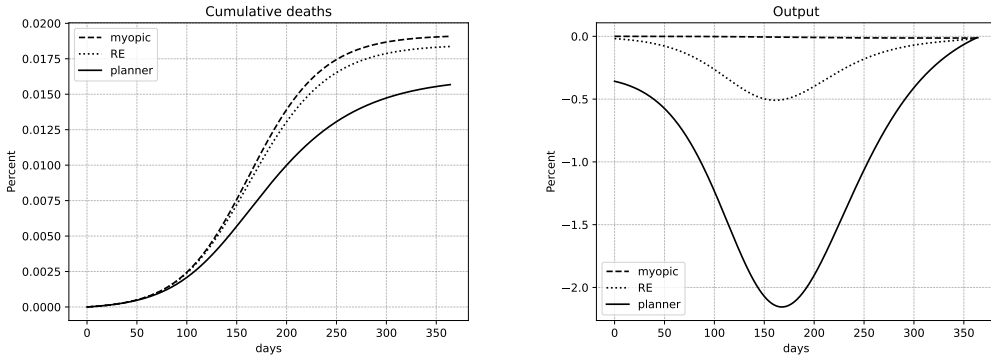
### B.3 SARS simulations, more details

To test our model with an epidemic that is substantially worse than covid-19, we use the SARS virus of 2002/2003 (severe acute respiratory syndrome coronavirus, SARS-CoV).

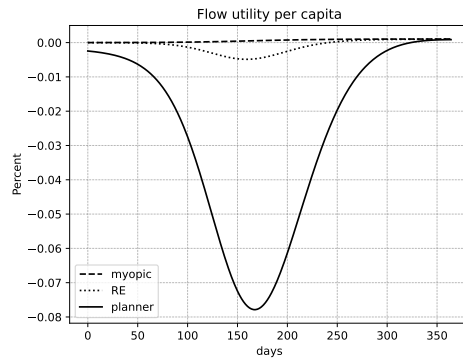
For the transmissability of SARS we use estimates from Petersen et al. (2020) and set  $R_0$  to 2.4. An age-related increase in mortality was observed also for SARS-CoV (although with a far greater case fatality). In Hong Kong, the case fatality due to SARS-CoV was 0% for age group 0-24 years, 6% for those aged 25-44 years, 15% for those aged 45-64 years, and 52% for people who were 65 years and older (Petersen et al. (2020)). We set the infection fatality rate to 8% for the group we define as young (15 to 60) and 45% for the group we define as old (above 60).<sup>6</sup>

SARS also has a slightly faster incubation period, so for average number of days until recover we use 12 days. In terms of overcrowding of hospitals, we assume that there is no overcrowding effect in the hospitals that could elevate the IFR even further.

<sup>6</sup>In the case of SARS, the difference between the case fatality rate and the infection fatality rate is small.



(a) Cumulative deaths under the three different flu scenarios. (b) Output drop under the three different flu scenarios.



(c) Drop in flow utility under the three different flu scenarios.

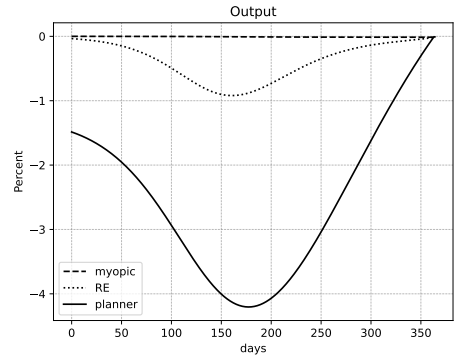
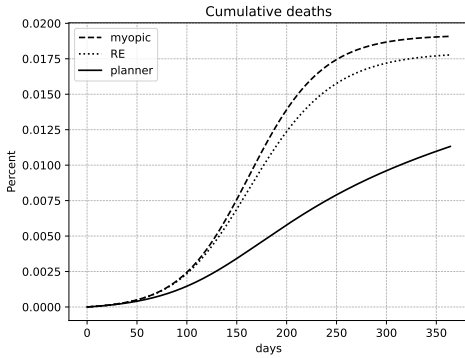
FIGURE B.3. Comparing the three different flu scenarios with a *low value of a statistical life* assumption.

*Results SARS* Figure B.6 shows the evolution of the SARS epidemic in the myopic market allocation, the rational-expectations competitive equilibrium, and the social planner's allocation under the assumption that a cure arrives after one year exactly.<sup>7</sup> Again, the epidemic under the myopic market allocation is close to standard SIR dynamics. Many people rapidly get infected. In the case of rational expectations, the behavior is qualitatively different. SARS is dangerous enough to make people so scared of being infected that they stay away from infectious activities voluntarily to a high extent.

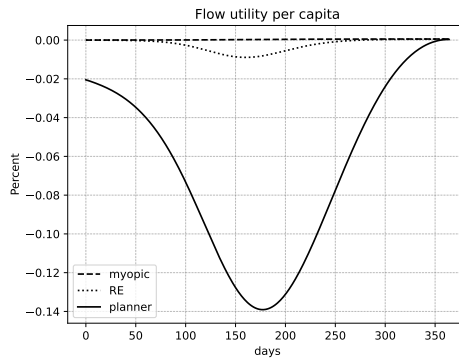
A social planner would lower the amount of infectious activities even more. In the case of a social planner, the epidemic is not allowed to take off at all, as Figure B.6c shows (we did not forget to plot the curve in this graph!).

As Figure B.7 shows, the results from the three scenarios are very different. The death toll is high in the myopic scenario, as expected. In the scenario with rational expecta-

<sup>7</sup>We only show the results for a low value of a statistical life, results from assuming a high value of a statistical life are very similar.



(a) Cumulative deaths under the three different flu scenarios. (b) Output drop under the three different flu scenarios.

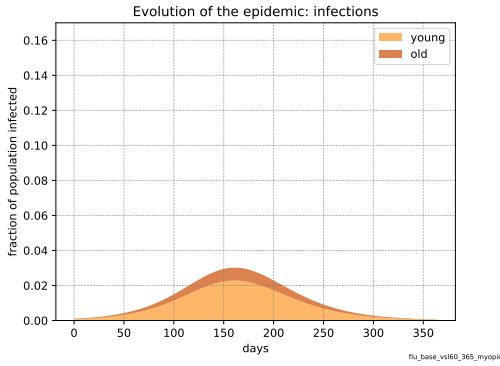


(c) Drop in flow utility under the three different flu scenarios.

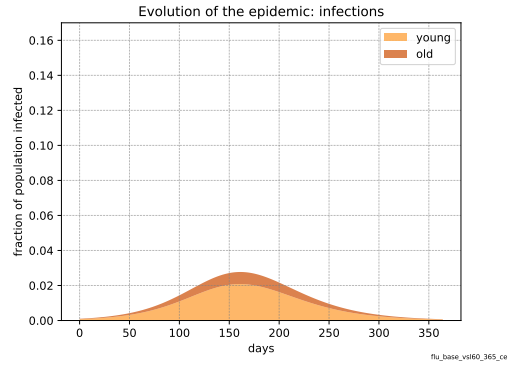
FIGURE B.4. Comparing the three different flu scenarios with a *high* value of a statistical life assumption.

tions, the number of deaths is reduced by more than 90%, and the social planner would reduce the number of deaths even more, as shown in Figure B.7a.

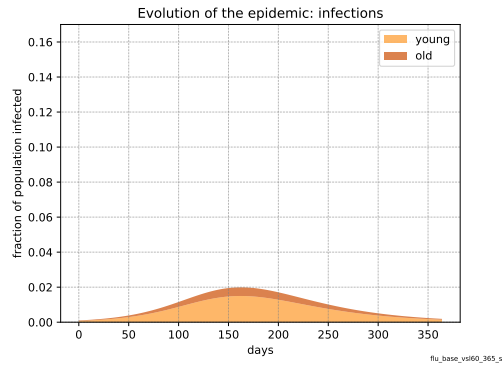
Figures B.7b and B.7c highlight the difference in strategy taken by a social planner compared to the rational-expectations equilibrium. A social planner would quickly lower the amount of infectious activities to get the epidemic under control, and would thereafter not have to reduce the activities as much. In the rational-expectations competitive equilibrium people would carry on with their activities until the number of infected is too high in the economy. Then people become afraid of becoming infected, and reduce their activities. Hence, in this scenario, the effective reproduction number is around 1 all the time for the rational expectation equilibrium. The annual drop in output in the rational-expectations scenario is 26.2 percent, which should be compared to the social-planner scenario, in which it is 23.9 percent. Thus, the social planner achieves not only less deaths, but also a smaller drop in output, by setting in “lock-down” measures early, and by doing so getting the epidemic under control at an early stage.



(a) The evolution of a seasonal flu under the myopic market allocation.



(b) The evolution of a seasonal flu in rational-expectations competitive equilibrium.



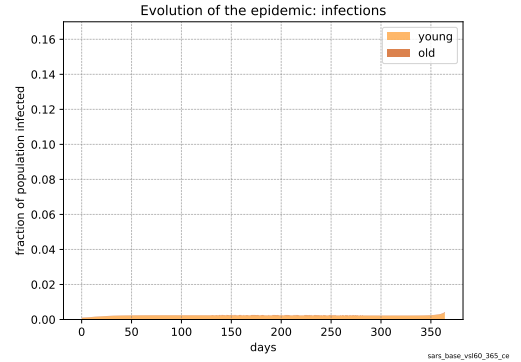
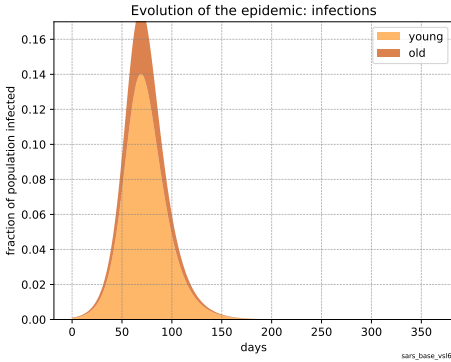
(c) The evolution of a seasonal flu under the social planner's allocation.

FIGURE B.5. The evolution of a seasonal flu under the social planner's allocation and the two different market allocations for the *low value of a statistical life* assumption.

The same type of qualitative effect, that the effective reproduction number hovers around 1 in a rational expectations scenario, is also reported by [Farboodi et al. \(2021\)](#) and [Bognanni et al. \(2020\)](#). The intuition behind the result is as follows. On one hand, the precautionary behavior is increasing in the infection risk, which is increasing in the number of infected. On the other hand, the number of infected is decreasing in the strength of the precautionary response. The infection rate therefore stabilizes around a level which is consistent with the precautionary behavior.

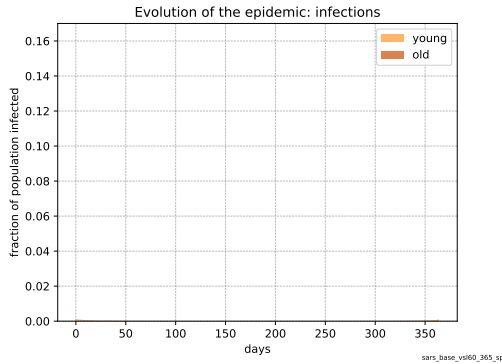
In our calibration of the covid-19 epidemic, we do not find that the effective reproduction number stabilizes around 1 in the rational-expectations competitive equilibrium. Including age heterogeneity in the model is important for our result. For the young, the risk of a covid infection does not provide a sufficiently strong motive for a precautionary response to stabilize the infection rate.





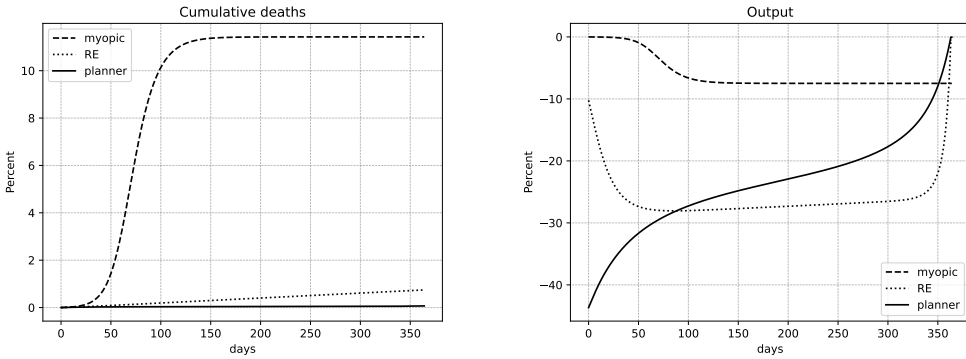
(a) The evolution of a SARS epidemic under the myopic market allocation.

(b) The evolution of a SARS epidemic under the rational expectations competitive equilibrium.

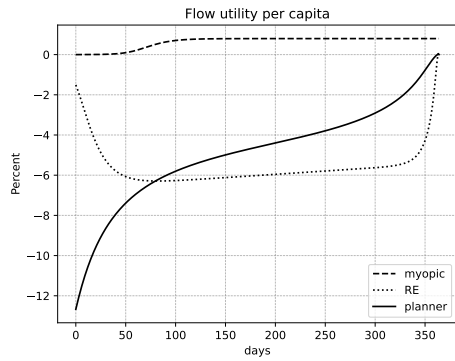


(c) The evolution of a SARS epidemic under the social planner's allocation.

FIGURE B.6. The evolution of a SARS epidemic under the social planner's allocation and the two different market allocations.



**(a)** Cumulative deaths under the three different SARS scenarios. **(b)** Output drop under the three different SARS scenarios.



**(c)** Drop in flow utility under the three different SARS scenarios.

FIGURE B.7. Comparing the three different SARS scenarios.

## APPENDIX: REFERENCES

- Biggerstaff, Matthew, Simon Cauchemez, Carrie Reed, Manoj Gambhir, and Lyn Finelli (2014), “Estimates of the reproduction number for seasonal, pandemic, and zoonotic influenza: a systematic review of the literature.” *BMC infectious diseases*, 14 (1), 480. [10]
- Bognanni, Mark, Doug Hanley, Daniel Kolliner, and Kurt Mitman (2020), “Economic activity and COVID-19 transmission: Evidence from an estimated economic-epidemiological model.” [16]
- Dushoff, Jonathan, Joshua B Plotkin, Cecile Viboud, David JD Earn, and Lone Simonsen (2006), “Mortality due to influenza in the United States—An annualized regression approach using multiple-cause mortality data.” *American Journal of Epidemiology*, 163 (2), 181–187. [12]
- Farboodi, Maryam, Gregor Jarosch, and Robert Shimer (2021), “Internal and external effects of social distancing in a pandemic.” *Journal of Economic Theory*, 196, 105293. [16]
- Faust, Jeremy Samuel and Carlos Del Rio (2020), “Assessment of deaths from COVID-19 and from seasonal influenza.” *JAMA Internal Medicine*. [10]
- Petersen, Eskild, Marion Koopmans, Unyeong Go, Davidson H Hamer, Nicola Petrosillo, Francesco Castelli, Merete Storgaard, Sulien Al Khalili, and Lone Simonsen (2020), “Comparing SARS-CoV-2 with SARS-CoV and influenza pandemics.” *The Lancet Infectious Diseases*. [11, 13]
- Rolfes, Melissa A, Ivo M Foppa, Shikha Garg, Brendan Flannery, Lynnette Brammer, James A Singleton, Erin Burns, Daniel Jernigan, Sonja J Olsen, Joseph Bresee, et al. (2018), “Annual estimates of the burden of seasonal influenza in the United States: a tool for strengthening influenza surveillance and preparedness.” *Influenza and other respiratory viruses*, 12 (1), 132–137. [12]